Validity of temperature and time equivalence in metallic glasses during shear deformation

Mareike Zink,[1] K. Samwer,[1] W. L. Johnson,[2] and S. G. Mayr[1,*]
[1]*I. Physikalisches Institut, Georg-August-Universität Göttingen, Friedrich-Hund-Platz 1, 37077 Göttingen, Germany*
[2]*138-78 Keck Laboratory of Engineering, California Institute of Technology, Pasadena, California 91125, USA*
(Received 22 April 2006; revised manuscript received 22 May 2006; published 5 July 2006)

Competing internal and external time scales, which are determined by temperature and experimental sampling time—viz., reciprocal frequency—respectively, are essentials for understanding the physics of glasses and the glass transition. A temperature increase should ideally affect thermally activated phenomena in a similar manner as an increase of sampling time at constant temperature. We investigate the validity of this empirical principle by its manifestations in mechanical properties—viz., the temperature and strain rate dependence of the shear modulus and yield stress of a CuTi model glass in molecular dynamics computer simulations. In equivalence to the temperature-dependent glass transition, we identify a shear-rate-dependent glass transition below a certain threshold. Beyond that, deviations occur in a highly non-Newtonian regime.

DOI: 10.1103/PhysRevB.74.012201 PACS number(s): 64.70.Pf, 02.70.Ns, 62.20.Dc

The glass transition—one of the few remaining mysteries of solid-state physics—has attracted the interest of numerous researchers during the past century (e.g., Refs. 1–4 and references therein) and nevertheless still remains unclear in central aspects. It is, however, well established that the relation of experimental sampling time—viz., reciprocal frequency—and internal relaxation time of a disordered system plays a key role for the question, whether it appears as a liquid or solid.[1] In particular, a glassy system should show a glass transition, once the experimental sampling time exceeds the internal relaxation time.[5] However, the time frame in which this picture is valid remains unclear—except that it should at least break down, once the experimental sampling time scale reaches the order of the reciprocal Debye frequency. Tightly related are the issues of anelasticity in glasses and crystals,[6] as well as "aging" processes in glasses,[7] which are basically linked to the fact that the glassy state itself in a strict sense is not a thermodynamic phase but depends on the history of the system. Generally the manifestations of these phenomena are experimentally accessible in macroscopic properties, such as plastic and elastic deformation.[8,9] Metallic glasses[10] are a paradigm to address these questions, particularly due to their structural simplicity—at least when compared to their polymeric counterparts. Despite recent progress in processing bulk metallic glasses, which has opened new experimental windows for investigating mechanical and thermal properties,[11–13] molecular dynamics (MD) computer simulations continue to be an increasingly powerful and promising tool to access glassy dynamics from atomic scales up to mesoscopic levels.

In the present work, we employ MD studies of the model glass, CuTi, to first investigate the sampling time-temperature equivalence, which will result in an improved understanding of the time- and temperature-dependent glass transition, as well as glassy dynamics in general. The studies are inspired by the cooperative shear model by Johnson and Samwer,[14,15] which gives a detailed picture for the microscopic dynamics and predicts the impact on macroscopic constants during shearing. In particular, it includes the idea that thermally activated processes can be described within a potential energy landscape (PEL),[16] which deforms under the influence of an applied shear stress, and, moreover, proposes that macroscopic shear deformation is mediated by nanoscale shear transformation zones (STZ's).[17–20] Within this picture, the local shear modulus of an STZ is determined by the curvature of the potential energy density as a function of strain—viz., $G=\phi''=\frac{\partial^2\phi}{\partial\gamma^2}$. Similarly, the maximum local shear stress at the yielding point is given by $\tau_{c,\mathrm{local}}=\phi'|_{max}$. It is a second aim of our present studies to countercheck the consequences of these predictions of the model on macroscopic constants. Both aims are achieved by determining the temperature and shear rate dependence of the shear modulus and yield stress when applying pure shear strain in MD simulations.

We employ the interatomic embedded atom method (EAM) potential,[21] as parametrized by Sabochick and Lam,[22] for simulating a cell of 35 152 Cu and Ti atoms total. This potential agrees well with experimental data, particularly with respect to mechanical and thermal properties in the crystalline as well as the amorphous phase, as shown previously.[23–25] Berendsen thermostats and barostats[26] are employed to maintain isothermal and isobaric conditions, respectively. Initially the atoms are arranged in a cubic simulation cell of $L\approx 80$ Å side length, while periodic boundaries are applied in all directions at zero pressure. Amorphous cells are prepared by quenching the liquid phase from 4500 K down to 10 K, while we chose the quench rate through the glass transition low enough (0.1 K/ps) to ensure sufficient relaxation. By monitoring the volume change during quenching, we determine a glass transition temperature of $T_g^{quench}=610$ K, while $T_g^{heat}=850$ K is determined during temperature increase (1 K/ps). The latter heating rate is also applied to reach the base temperatures of the experiments, as discussed below. Before applying a shear strain to the system, the topmost ($+z$ direction) and bottommost ($-z$ direction) four atomic layers are fixed and the boundaries are opened in all spatial directions, while pressure control is disabled. We would like to emphasize that we purposely employ open boundaries, while simulating a reasonably large cell to exclude artifacts due to periodic boundary constraints on the one hand and open surfaces on the other. Afterwards, the open surfaces are relaxed for another 500 ps, and the radial distribution functions are calculated, which show the typical

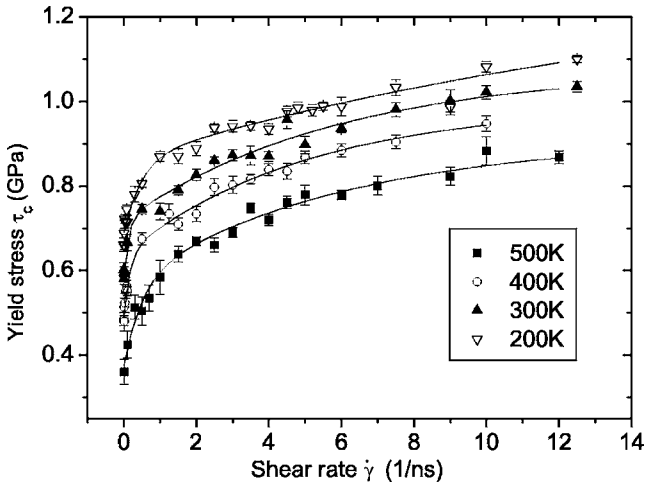

FIG. 1. Maximum shear stress at the yielding point—measured as a function of strain rate for various temperatures.

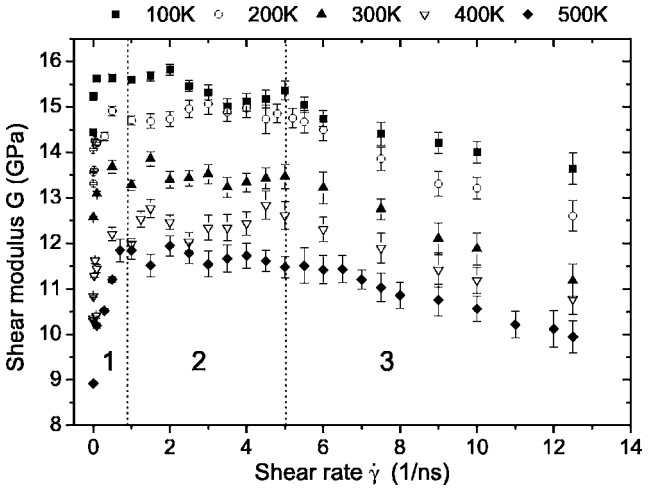

FIG. 2. Shear rate dependence of the effective shear modulus for various temperatures.

signatures of an amorphous metal. Shear strain is now applied by moving the topmost four atomic layers at constant velocity U in the $+y$ direction, which corresponds to a strain rate of $\dot{\gamma}=U/L$. The resulting shear stresses are determined from the virials. Strain rates of $0.005\times10^9\ \mathrm{s}^{-1}\leq\dot{\gamma}\leq15.0\times10^9\ \mathrm{s}^{-1}$ are applied, whereas higher rates interfere with the velocity of sound and lead to a destruction of the system by heterogeneous shear deformation of the cell, as expected. To exclude that our way of applying shear strains generates shock waves, which interfere with the shear deformation, we additionally sheared one typical cell with a rate of $1\times10^{10}\ \mathrm{s}^{-1}$ by moving *all* atoms corresponding to a uniform shear deformation of the cell. Identical results are obtained, independent of how the shear strains are applied, which confirms our approach.

The effective shear modulus G and the maximum shear stress at the yielding point of the total cell, τ_c, are determined from stress-strain curves. τ_c as a function of strain rate is given by Fig. 1. We empirically find an approximately exponential dependence of τ_c on $\dot{\gamma}$, which can be qualitatively understood by considering the microscopic relaxation dynamics: Prior to shearing, the configurational coordinates of the system locally reside within minima of the PEL. The latter is modified due to an elastic energy contribution by stresses caused by the applied shear strain. While at low strain rates the system has sufficient time to thermally relax towards the new local minimum-energy configurations, high strain rates suppress thermal relaxation on time scales of $\gtrapprox 1/\dot{\gamma}$. Here only athermal effects remain possible.

This picture also helps to understand the effect of varying strain rates on the effective shear modulus, as shown in Fig. 2. When considering G as a function of strain rate $\dot{\gamma}$, it is possible to distinguish three different regimes, as indicated by the dotted lines in Fig. 2: (1) For *low strain rates* the time scales for thermally activated structural relaxation ("α process") τ_t are smaller than the reciprocal shear rate ($\tau_t\lessapprox 1/\dot{\gamma}$); the material flows similar to temperatures above T_g.[27] The effective shear modulus is dominated by thermal transitions into energetically favored configurations (viz., minima of the PEL), which are also the limiting factor for the yield stresses. (2) In cases of *medium strain rates* the rate of thermally activated relaxation events decreases dramatically, while increasing stress levels (towards the maximum yield stress of the CuTi system) lead to a reduction—and even vanishing—of the activation energy for reorientation. The effective shear modulus G reaches its maximum value and becomes independent of frequency, which is a characteristic of Newtonian flow.[12] Also in this regime, however, G remains smaller than the isoconfigurational shear modulus G_∞ (500 K) $\approx$ (44.7 $\pm$ 0.5) GPa, as determined from fluctuation-dissipation theorems.[28] (3) In the *high-strain-rate* regime, the available time to the system gets so short that strain localization and defects (or, equivalently, free volume) are generated, while thermal relaxation counteracts. This is reflected by a shear modulus, which becomes dependent on frequency again. In addition, the system is increasingly located between the potential energy minima and the saddle points of ϕ where $\phi''=0$. Here the curvature of ϕ is smaller than at the PEL minima and the shear modulus is addition-

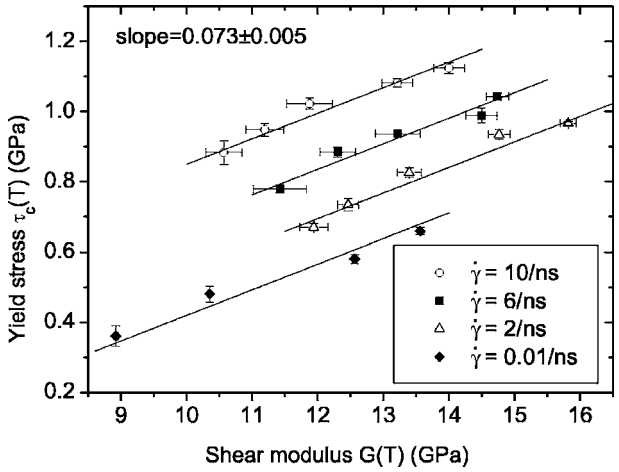

FIG. 3. Relation of shear stress at the yielding point $\tau_c(T)$ and shear modulus $G(T)$ at different temperatures. Every data point corresponds to a different temperature $T<T_g$ at the specified shear rate.

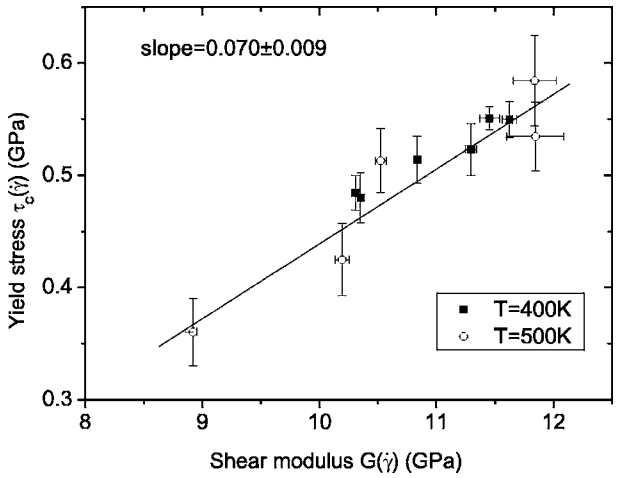

FIG. 4. Relation of shear stress at the yielding point $\tau_c(\dot{\gamma})$ and shear modulus $G(\dot{\gamma})$ at different strain rates, $\dot{\gamma} \leq 1/\mathrm{ns}$ [within regime (1) of Fig. 2]. Every data point corresponds to an individual shear rate at the specified temperature.

ally reduced, which is accompanied by non-Newtonian flow.

In all cases (1)–(3), increased thermal vibrations due to elevated temperatures further drive configurations out of their local minima due to any anharmonicity in the potential energy density, as characterized by the Debye-Grüneisen coefficient. This leads to a decrease of shear modulus with increasing temperature, as observed in Fig. 2. The transition from the liquidlike regime (1) to the solidlike regime (2) corresponds to a rate-dependent glass transition, similar to its temperature-dependent counterpart. The rate-dependent glass transition shifts to smaller strain rates as the temperature is decreased, as thermally activated processes are increasingly suppressed. This equivalence of temperature and sampling time breaks down at very high strain rates, where the crossover from (2) to (3) appears. The critical shear rates for this transition are not clear to determine from our data within the error bars of $G(\dot{\gamma})$. We expect, however, a shift to higher strain rates at higher temperatures, as elevated temperatures might facilitate the elimination of defects and disorder, which are created during shearing. The latter statement is corroborated by aging the glass: We find that the shear modulus for a CuTi simulation cell, after additional annealing at 400 K for another 10 ns, is comparable to the shear modulus of a cell at 300 K, which has not been additionally annealed before.

To investigate the influence of temperature and shear rate variation on the macroscopic constants, we plot $\tau_c(T)$ as a function of $G(T)$ (Fig. 3) and $\tau_c(\dot{\gamma})$ vs $G(\dot{\gamma})$ (Fig. 4). In analogy to Johnson and Samwer,[14] we find a universal yielding criterion for τ_c and G at those strain rates where thermally activated transitions occur:

$$\tau_c(T) = \gamma_{c,T} G(T) \quad \text{with} \quad \gamma_{c,T} = 0.073 \pm 0.005, \tag{1}$$

$$\tau_c(\dot{\gamma}) = \gamma_{c,\dot{\gamma}} G(\dot{\gamma}) \quad \text{with} \quad \gamma_{c,\dot{\gamma}} = 0.070 \pm 0.009. \tag{2}$$

It becomes clear that the changes of the shear modulus and yield stress upon variation of temperature (at fixed $\dot{\gamma}$) or shear rate (at fixed T) are equivalent, as indicated by identical slopes $\gamma_{c,T} = \gamma_{c,\dot{\gamma}}$. This means that the equilibrium distribution of STZ's is of the same kind as the strain-induced one. An increase in temperature with $\dot{\gamma}$=const leads to the same macroscopic behavior of the system as smaller strain rates and T=const. In this case, the temperature and strain rate can be used as equivalent parameters that influence elastic constants in glasses oppositely.

In cases of high strain rates where thermal activated transitions of STZ's are suppressed [regime (3) of Fig. 2], we find a yielding criterion by analyzing $G(\dot{\gamma})$ and $\tau_c(\dot{\gamma})$ for $\dot{\gamma} \geq 5/\mathrm{ns}$ similar to Fig. 4:

$$\tau_c(\dot{\gamma}) = \gamma'_{c,\dot{\gamma}} G(\dot{\gamma}) \quad \text{with} \quad \gamma'_{c,\dot{\gamma}} = -0.070 \pm 0.008. \tag{3}$$

Under these conditions, the opposite signs of $\gamma'_{c,\dot{\gamma}}$ and $\gamma_{c,T}$ suggest an equivalent impact of temperature (with $\dot{\gamma}$=const) and strain rate (with T=const), respectively, on the elastic properties. The self-consistent free-volume model proposed by Demetriou and Johnson[29] is suitable to understand this phenomenon qualitatively: Non-Newtonian flow due to high strain rates can be rationalized by the creation of free volume in the system. In this sense, the equivalence of the absolute values of $\gamma'_{c,\dot{\gamma}}$ and $\gamma_{c,T}$ indicates an equivalence of the free volume created by shearing and the volume change due to thermal expansion.

To conclude, the effective shear modulus of metallic glasses depends on the α-relaxation time of the system. For $\tau_t \lessapprox 1/\dot{\gamma}$ the system relaxes during shearing and flows homogeneously in time—just as above T_g. The shear modulus becomes frequency independent if τ_t exceeds $\approx 1/\dot{\gamma}$; viz., relaxation processes are suppressed and thermally activated configurational changes are inhibited. Even higher strain rates lead to softening due to local mechanical instabilities and defect generation; an increase in temperature is then equivalent to elevated strain rates.

In a nutshell, we have shown by systematic studies that, in fact, sampling time and temperature are equivalent and lead to the same mechanical response of amorphous systems, as long as local mechanical stability is maintained.

M.Z., K.S., and S.G.M. acknowledge financial support by the German DFG-SFB 602 and G.I.F., No. G-2103-1428.14/2004, as well as the GWDG (Gesellschaft für wissenschaftliche Datenverarbeitung Göttingen, Germany) for a grant of computing time.

*Author to whom correspondence should be addressed. Electronic address: smayr@uni-goettingen.de

[1] J. Zarzycki, *Glasses and the Vitreous State* (Cambridge University Press, Cambridge, England, 1982).
[2] S. R. Elliott, *Physics of Amorphous Materials* (Longman Scientific, London, 1990).
[3] C. A. Angell, Science **267**, 1924 (1995).
[4] J. F. Loeffler, Intermetallics **11**, 529 (2003).
[5] M. E. Cates and P. Sollich, Eur. Phys. J. B **10**, 705 (1999).
[6] A. S. Nowick and B. S. Berry, *Anelastic Relaxation in Crystalline Solids* (Academic Press, New York, London, 1972).
[7] Y. Hiki, T. Yagi, T. Aida, and S. Takeuchi, Mater. Sci. Eng., A **370**, 302 (2004).
[8] Q. Wang, J. M. Pelletier, Y. D. Dong, and Y. F. Ji, Mater. Sci. Eng., A **370**, 316 (2004).
[9] O. Henrich, F. Varnik, and M. Fuchs, J. Phys.: Condens. Matter **17**, S3625 (2005).
[10] W. L. Johnson, Mater. Res. Bull. **24**, 42 (1999).
[11] J. Lu, G. Ravichandran, and W. L. Johnson, Acta Mater. **51**, 3429 (2003).
[12] H. Kato, Y. Kawamura, A. Inoue, and H. S. Chen, Appl. Phys. Lett. **73**, 3665 (1998).
[13] J. Schroers, JOM **57**, 35 (2005).
[14] W. L. Johnson and K. Samwer, Phys. Rev. Lett. **95**, 195501 (2005).
[15] M. Zink, K. Samwer, W. L. Johnson, and S. G. Mayr, Phys. Rev. B **73**, 172203 (2006).
[16] P. G. Debenedetti and F. H. Stilliger, Nature (London) **410**, 259 (2001).
[17] A. S. Argon, Acta Metall. **27**, 47 (1979).
[18] C. A. Schuh and A. C. Lund, Nat. Mater. **2**, 449 (2003).
[19] M. L. Falk and J. S. Langer, Phys. Rev. E **57**, 7192 (1998).
[20] M. L. Falk, J. S. Langer, and L. Pechenik, Phys. Rev. E **70**, 011507 (2004).
[21] M. S. Daw and M. I. Baskes, Phys. Rev. B **29**, 6443 (1984).
[22] M. J. Sabochick and N. Q. Lam, Phys. Rev. B **43**, 5243 (1991).
[23] S. G. Mayr, Y. Ashkenazy, K. Albe, and R. S. Averback, Phys. Rev. Lett. **90**, 055505 (2003).
[24] S. G. Mayr, Phys. Rev. B **71**, 144109 (2005).
[25] S. Vauth and S. G. Mayr, Appl. Phys. Lett. **86**, 061913 (2005).
[26] H. J. C. Berendsen, J. P. M. Postma, W. F. van Gunsteren, A. DiNola, and J. R. Haak, J. Chem. Phys. **81**, 3684 (1984).
[27] A. S. Bains, C. A. Gorgon, A. V. Granato, and R. B. Schwarz, J. Alloys Compd. **310**, 20 (2000).
[28] M. Parrinello and A. Rahman, J. Chem. Phys. **76**, 2662 (1982).
[29] M. D. Demetriou and W. L. Johnson, Mater. Sci. Eng., A **375-377**, 270 (2004).